Eur. Phys. J. B **7**, 635–643 (1999)

THE EUROPEAN PHYSICAL JOURNAL B

EDP Sciences

A model for anomalous directed percolation

H. Hinrichsen[1,a] and M. Howard[2]

[1] Max-Planck-Institut für Physik komplexer Systeme, Nöthnitzer Straße 38, 01187 Dresden, Germany
[2] CATS, The Niels Bohr Institute, Blegdamsvej 17, 2100 Copenhagen Ø, Denmark

Received: 4 September 1998 / Accepted: 22 September 1998

Abstract. We introduce a model for the spreading of epidemics by long-range infections and investigate the critical behaviour at the spreading transition. The model generalizes directed bond percolation and is characterized by a probability distribution for long-range infections which decays in d spatial dimensions as $1/r^{d+\sigma}$. Extensive numerical simulations are performed in order to determine the density exponent β and the correlation length exponents $\nu_\parallel$ and $\nu_\perp$ for various values of σ. We observe that these exponents vary continuously with σ, in agreement with recent field-theoretic predictions. We also study a model for pairwise annihilation of particles with algebraically distributed long-range interactions.

PACS. 05.70.Ln Nonequilibrium thermodynamics, irreversible processes – 64.60.Ak Renormalization-group, fractal, and percolation studies of phase transitions – 64.60.Ht Dynamic critical phenomena

1 Introduction

Spreading processes are often encountered in nature in situations as diverse as epidemics [1,2], catalytic reactions [3], forest fires [4], and transport in random media [5,6]. Depending on the particular environmental conditions, the spreading process may either continue to spread over the whole population or die out after some time. The essential features of this transition between survival and extinction of the spreading agent may be described by simple stochastic lattice models, which mimic the spreading mechanism by certain probabilistic rules. Usually such models incorporate two competing processes, namely spreading (infection) of nearest neighbors and spontaneous recovery (healing), with or without immunization. The spreading properties depend on the relative rates of the two processes. For example, if the rate for infection is very low, the spreading agent will disappear after some time and the system becomes trapped in an inactive state (or set of states) which is usually referred to as the *absorbing* state of the model. On the other hand, if infections occur more frequently, the spreading process may survive for a very long time. The main theoretical interest in these models stems from the fact that the phase transition from the fluctuating active phase into the non-fluctuating absorbing state is continuous, and characterized by universal scaling laws associated with certain critical exponents. As in equilibrium statistical mechanics, these exponents allow one to categorize different lattice models into universality classes. Each of these universality classes then corresponds to a specific underlying field theory.

The most important universality class for spreading transitions with short-range interactions is Directed Percolation (DP) [7], as described by Reggeon field theory [8–10]. In fact, DP covers the majority of phase transitions from a fluctuating active phase into absorbing states. The fundamental properties of DP have been expressed as a conjecture in references [10,11]. Accordingly a spreading transition belongs to the DP class if (a) the absorbing state is unique, (b) the active phase is characterized by a one-component positive order parameter, (c) there are no other symmetries of the physical system except for spatio-temporal translation and spatial reflection invariance, (d) there is no frozen disorder, and (e) the dynamical rules involve only short-range interactions.

In many realistic spreading processes, however, short-range interactions do not appropriately describe the underlying transport mechanism. This situation emerges, for example, when an infectious disease is transported by insects. The motion of the insects is typically not a random walk, rather one observes occasional flights over long distances before the next infection occurs. Similar phenomena are expected when the spreading agent is subjected to a turbulent flow. It is intuitively clear that occasional spreading over long distances will significantly alter the spreading properties. On a theoretical level such a *super-diffusive* motion may be described by Lévy flights [6], *i.e.*, by uncorrelated random moves over algebraically distributed distances.

Anomalous directed percolation, as originally proposed by Mollison [1] in the context of epidemic spreading, is a generalization of DP in which the spreading agent

[a] e-mail: hinrichs@mpipks-dresden.mpg.de

performs Lévy flights. This means that the distribution of the spreading distance r is given by

$$P(r) \sim 1/r^{d+\sigma}, \qquad (\sigma > 0), \tag{1}$$

where d denotes the spatial dimension of the system. The exponent σ is a free parameter that controls the characteristic shape of the distribution. It should be emphasized that σ does *not* introduce any new length scale, rather it changes the scaling properties of the underlying (anomalous) diffusion process. We are particularly interested in the critical properties of anomalous DP close to the phase transition. As in the case of ordinary DP, we expect anomalous DP to be characterized by the universal critical exponents β, $\nu_\perp$, and $\nu_\parallel$. The exponent β is related to the order parameter, the density of active sites n. Since the DP process is controlled by a single parameter p, with the phase transition taking place at $p = p_c$, then close to this transition in the active phase n vanishes as $n \sim (p - p_c)^\beta$. At the same time, we expect the spatial and temporal correlation lengths $\xi_\perp$ and $\xi_\parallel$ to diverge as $\xi_\perp \sim |p - p_c|^{-\nu_\perp}$ and $\xi_\parallel \sim |p - p_c|^{-\nu_\parallel}$, respectively, on *both* sides of the transition. Theoretically, one is interested in the dependence of these exponents on σ, whether the exponents are independent from one another, and how they cross over to the exponents of ordinary DP. Some time ago Grassberger [12] claimed that the critical exponents of anomalous DP should depend continuously on the control exponent σ. This was confirmed by estimations of the exponent β based on a coherent anomaly method [13]. Very recently this work has been considerably clarified and extended by Janssen *et al.* [14], who have presented a comprehensive field-theoretic renormalization group (RG) calculation for anomalous spreading processes with and without immunization. The aim of the present work is to verify their results numerically. To this end we introduce a model for anomalous DP which generalizes directed bond percolation. In contrast to previously studied models [15,16] we do not introduce an upper cutoff for the flight distance r, and hence finite size effects are drastically reduced. Extensive numerical simulations are performed in order to determine the critical exponents, which are found to compare favourably with the field-theoretic predictions.

The paper is organized as follows. In Section 2 we first review the known field-theoretic results. In Section 3 we introduce a lattice model for anomalous DP and discuss the role of finite size effects. In Section 4 the numerical results are presented and compared with the field-theoretic predictions. We also discuss the case of anomalous pair annihilation in Section 5.

2 Field-theoretic predictions

In this section we will summarize some of the field-theoretic results which have been derived in reference [14]. First of all let us recall that the Langevin equation for ordinary DP [10] is given by

$$\frac{\partial}{\partial t} n(\mathbf{x},t) = (\tau + D_N \nabla^2)\, n(\mathbf{x},t) - \lambda\, n^2(\mathbf{x},t) + \zeta(\mathbf{x},t), \tag{2}$$

where the constant τ controls the balance between offspring production and self-destruction, and plays the role of the deviation $p - p_c$ from the critical percolation probability. The infection of nearest neighbors is represented by the diffusion operator ∇^2, while the nonlinear term incorporates the exclusion principle on the lattice. The fluctuations are taken into account by adding a multiplicative Gaussian noise field $\zeta(\mathbf{x},t)$ which is defined by the correlations

$$\langle \zeta(\mathbf{x},t)\zeta(\mathbf{x}',t')\rangle = 2\Gamma\, n(\mathbf{x},t)\, \delta^d(\mathbf{x}-\mathbf{x}')\delta(t-t'). \tag{3}$$

In order to generalize this Langevin equation to the case of anomalous DP, the short-range diffusion has to be replaced by a non-local integral expression which describes long-range spreading according to the probability distribution $P(r)$:

$$\frac{\partial}{\partial t} n(\mathbf{x},t) = \tau\, n(\mathbf{x},t) - \lambda\, n^2(\mathbf{x},t) + \zeta(\mathbf{x},t) + D \int d^d x'\, P(|\mathbf{x}-\mathbf{x}'|)[n(\mathbf{x}',t) - n(\mathbf{x},t)]. \tag{4}$$

The two contributions in the integrand describe gain and loss processes, respectively. Keeping the most relevant terms in a small momentum expansion, this equation may be written as [14]

$$\frac{\partial}{\partial t} n(\mathbf{x},t) = \Big(D_N \nabla^2 + D_A \nabla^\sigma + \tau\Big) n(\mathbf{x},t) - \lambda n^2(\mathbf{x},t) + \zeta(\mathbf{x},t), \tag{5}$$

where the noise correlations are assumed to be the same as in equation (3). D_N and D_A are the rates for normal and anomalous diffusion, respectively. The anomalous diffusion operator ∇^σ describes moves over long distances and is defined through its action in momentum space

$$\nabla^\sigma\, e^{i\mathbf{k}\cdot\mathbf{x}} = -k^\sigma\, e^{i\mathbf{k}\cdot\mathbf{x}}, \tag{6}$$

where $k = |\mathbf{k}|$. The standard diffusive term $D_N \nabla^2$ takes into account the short range component of the Lévy distribution. Note that even if this term were not initially included, it would still be generated under renormalization of the theory.

Before summarizing the field-theoretic results, let us first consider the mean-field approximation. As in ordinary DP the mean-field dynamic phase transition occurs at $\tau = 0$, where gain and loss processes balance one another. For $\tau < 0$, the particle density decays exponentially quickly towards $n = 0$, which is the absorbing state of the system. However, for $\tau > 0$, the stable stationary state now has the non-zero particle density $n = \tau/\lambda$. Since τ plays the role of $p - p_c$, the mean field density exponent is $\beta^{MF} = 1$.

The scaling exponents $\nu_\perp$ and $\nu_\parallel$ can be derived from an inspection of equation (5). For $\sigma < 2$, we see that

$$\xi_\perp \sim |\tau|^{-\nu_\perp}, \qquad \nu_\perp^{MF} = 1/\sigma, \tag{7}$$

and the characteristic time diverges according to

$$\xi_\parallel \sim |\tau|^{-\nu_\parallel}, \qquad \nu_\parallel^{MF} = 1. \tag{8}$$

As expected, for $\sigma \geq 2$, these exponents cross over smoothly to the ordinary DP exponents. Note that the mean field result demonstrates that $\nu_\perp$ varies continuously with σ.

The mean field approximation is expected to be quantitatively accurate above the upper critical dimension. For $d \leq d_c$, however, fluctuation effects have to be taken into account. The fluctuation corrections to the critical exponents can be computed by a field-theoretic RG calculation. Using standard techniques, the Langevin equation (5) can be rewritten as an effective action:

$$S[\bar\psi,\psi] = \int d^dx\ dt\ \Big[\bar\psi(\partial_t - \tau - D_N\nabla^2 - D_A\nabla^\sigma)\psi + \frac{g}{2}(\bar\psi\psi^2 - \bar\psi^2\psi)\Big]. \tag{9}$$

Simple power counting on this action reveals that the upper critical dimension is $d_c = 2\sigma$, below which fluctuation effects become important. In the above action the field $\psi(\mathbf{x},t)$ can be identified with the coarse-grained particle density field $n(\mathbf{x},t)$ [17] and $\bar\psi(\mathbf{x},t)$ is the corresponding response field. The expression in equation (9) differs from the usual action of Reggeon field theory [8–10] by the addition of a term representing anomalous diffusion.

The field-theoretic RG calculation in reference [14] employs Wilson's momentum shell renormalization group recursion relations in order to determine the critical exponents. The authors of the present work have independently performed similar calculations based on dimensional regularization which are fully consistent with reference [14]. In the following we summarize the main results. The critical exponents to one-loop order in $d = 2\sigma - \epsilon$ dimensions are given by

$$\begin{aligned}
\beta &= 1 - \frac{2\epsilon}{7\sigma} + O\left(\epsilon^2\right), \\
\nu_\perp &= \frac{1}{\sigma} + \frac{2\epsilon}{7\sigma^2} + O\left(\epsilon^2\right), \\
\nu_\parallel &= 1 + \frac{\epsilon}{7\sigma} + O\left(\epsilon^2\right), \\
z &= \frac{\nu_\parallel}{\nu_\perp} = \sigma - \epsilon/7 + O\left(\epsilon^2\right).
\end{aligned} \tag{10}$$

Moreover, it can be shown that the hyperscaling relation

$$\theta + 2\delta = d/z \qquad (\delta = \beta/\nu_\parallel), \tag{11}$$

for the so-called critical initial slip exponent θ [18], holds for arbitrary values of σ. The exponent θ (which is also sometimes denoted by η in the literature) describes the initial increase in the number of active particles $N(t)$ for critical systems starting from initial states at very low density, *i.e.* where we have $N(t) \sim t^\theta$. The critical initial slip plays an important role in dynamical Monte-Carlo simulations (see Sect. 4). To one-loop order, θ and δ are given by

$$\theta = \frac{\epsilon}{7\sigma} + O\left(\epsilon^2\right), \qquad \delta = 1 - \frac{3\epsilon}{7\sigma} + O\left(\epsilon^2\right). \tag{12}$$

Finally, thanks to the fact that D_A does not get renormalized, one can prove the *exact* scaling relation

$$\nu_\parallel - \nu_\perp(\sigma - d) - 2\beta = 0. \tag{13}$$

The fact that D_A does not get renormalized means that anomalous DP is described by *two* rather than three independent critical exponents. The scaling relation (13) has a further surprising consequence. Assuming that β, $\nu_\perp$ and $\nu_\parallel$ change continuously with σ, then for fixed d, it predicts the value σ_c where the system should cross over to ordinary DP (assuming the crossover is smooth). To this end one simply has to insert the numerically known values of the DP exponents into equation (13). Surprisingly one obtains $\sigma_c = 2.076\,6(2)$ in one, $\sigma_c \simeq 2.2$ in two, and $\sigma_c = 2 + \tilde\epsilon/12$ in $d = 4 - \tilde\epsilon$ spatial dimensions. Thus the crossover takes place at $\sigma_c > 2$ which collides with the intuitive argument that the anomalous diffusion operator ∇^σ should only be relevant if $\sigma < 2$. But, as pointed out in reference [14], this naive argument may be wrong in an interacting theory where the critical behaviour is determined by a nontrivial fixed point of an RG transformation. Rather the field-theoretic calculation predicts that anomalous diffusion is still relevant in the range $2 \leq \sigma < \sigma_c(d)$ for $d < 4$. This prediction seems to be additionally surprising since the operators for anomalous and ordinary diffusion ∇^σ and ∇^2 are expected to coincide for $\sigma = 2$. However, one can show that for $\sigma = 2$ the most relevant terms in a small momentum expansion of equation (4) also contain a logarithmic correction of the form $-k^2 \log k$. Therefore anomalous and ordinary diffusion are indeed different in that case, supporting the view that long-range spreading might be relevant in the regime $2 \leq \sigma < \sigma_c$. Unfortunately, the numerical simulations presented in Section 4 are not accurate enough to confirm this prediction.

Another interesting aspect of anomalous DP is that σ can be chosen in such a way that the critical dimension $d_c = 2\sigma$ approaches the actual physical dimension at which the simulations are performed (see Sect. 4). Even in one spatial dimension this allows us to verify the one-loop results (10). For example, if $\sigma = 1/2 + \mu$, the critical dimension of the system is $d_c = 1 + 2\mu$ and hence the exponents in a 1+1-dimensional system change to first order

in μ as

$$\begin{aligned}\beta &= 1 - 8\mu/7 + O\left(\mu^2\right), \\ \nu_\perp &= 2 - 12\mu/7 + O\left(\mu^2\right), \\ \nu_\parallel &= 1 + 4\mu/7 + O\left(\mu^2\right), \\ z &= 1/2 + 5\mu/7 + O\left(\mu^2\right), \\ \delta &= 1 - 12\mu/7 + O\left(\mu^2\right), \\ \theta &= 4\mu/7 + O\left(\mu^2\right). \end{aligned} \tag{14}$$

In Section 4 we shall demonstrate that this initial change of the exponents is indeed observed in numerical simulations.

3 A lattice model for anomalous directed percolation

Anomalous DP was first studied numerically by Albano [15] who introduced a model for branching-annihilating random walks in which the particles performed Lévy flights. However, his estimates for the critical exponents were rather inconclusive, in particular they violated the scaling relation (13) and even the mean-field limit was not correctly reproduced. In reference [14] it was suspected that these problems could have originated in the truncation of the flight distances at some upper cutoff, usually at the system size. The upper cutoff effectively suppressed long range motion and hence DP-like behaviour was amplified. A systematic finite size analysis of a similar model confirms this point of view and shows that even on a lattice with 10^4 sites finite-size effects are still extremely dominant.

Similar problems were also encountered in a more recent study of a generalized Domany-Kinzel model with long range interactions [16]. In this case an upper cutoff for $P(r)$ was also introduced (by defining transition probabilities $w(S_i^t|S^{t-1})$ in which the sum over the spreading distance for a system with N sites is truncated at $N/2$). It was reported that the percolation threshold depended on the system size and varied by more than 20%. However, it seems that this unusual drift of p_c is actually related to extremely strong finite size effects.

In order to minimize finite size effects, we introduce a model in which the probability distribution for long-range spreading is not truncated from above. As in the case of ordinary directed bond percolation, our model is defined on a tilted square lattice and evolves by parallel updates. A binary variable $s_i(t)$ is attached to each lattice site i. $s_i = 1$ means that the site is active (infected) whereas $s_i = 0$ denotes an inactive (healthy) site. Although the model may be defined in arbitrary spatial dimensions, we will focus here on the 1+1-dimensional case. The dynamical rules (see Fig. 1) depend on two parameters, namely the control exponent $\sigma > 0$ and the bond probability $0 \leq p \leq 1$. For a given configuration $\{s_i(t)\}$ at time t, the next configuration $\{s_i(t+1)\}$ is constructed as follows. First the new configuration is initialized by setting

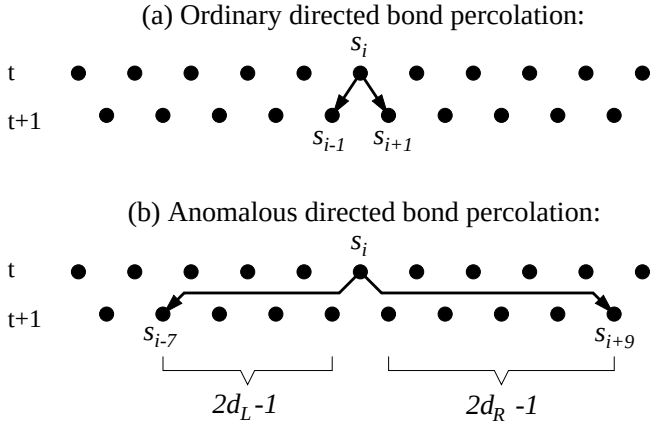

Fig. 1. Dynamical rules for (a) ordinary directed bond percolation and (b) the present model with algebraically distributed distances. d_L and d_R are defined in the text.

$s_i(t+1) := 0$. Then a loop over all active sites i in the previous configuration is executed. This loop consists of the following steps:

1. Generate two random numbers z_L and z_R from a flat distribution between 0 and 1.
2. Define two real-valued spreading distances $r_L = z_L^{-1/\sigma}$ and $r_R = z_R^{-1/\sigma}$, for spreading to the left (L) and to the right (R). The corresponding integer spreading distances d_L and d_R are defined as the largest integer numbers that are smaller than r_L and r_R, respectively. If d_L or d_R exceed the allowed range for integer numbers we go back to step 1.
3. Generate two further random numbers y_L and y_R drawn from a flat distribution between 0 and 1, and assign $s_{i+1-2d_L}(t+1) := 1$ if $y_L < p$, and $s_{i-1+2d_R}(t+1) := 1$ if $y_R < p$, respectively. In finite systems the arithmetic operations in the indices are carried out modulo L by assuming periodic boundary conditions, *i.e.* $s_i \equiv s_{i\pm L}$.

The model includes two special cases. For $\sigma \to \infty$ it reduces to ordinary directed bond percolation with $p_c \simeq 0.6447$. On the other hand, for $\sigma \to 0$ the interaction becomes totally random. In that case the model is exactly solvable and the transition takes place at $p_c = 1/2$. In between, the spreading properties of the model change drastically, as illustrated in Figure 2.

As can be easily verified, the assignment $r = z^{-1/\sigma}$ reproduces the normalized probability distribution

$$P(r) = \begin{cases} \sigma/r^{1+\sigma} & \text{if} \quad r > 1, \\ 0 & \text{otherwise.} \end{cases} \tag{15}$$

As usual the distribution has a lower cutoff at $r_{min} = 1$, which represents the lattice spacing. But in contrast to previously studied models, no upper cutoff is introduced and therefore almost arbitrarily large spreading distances may be generated (limited only by the maximal range of 64-bit integer numbers). In finite systems the target site is determined by assuming periodic boundary conditions,

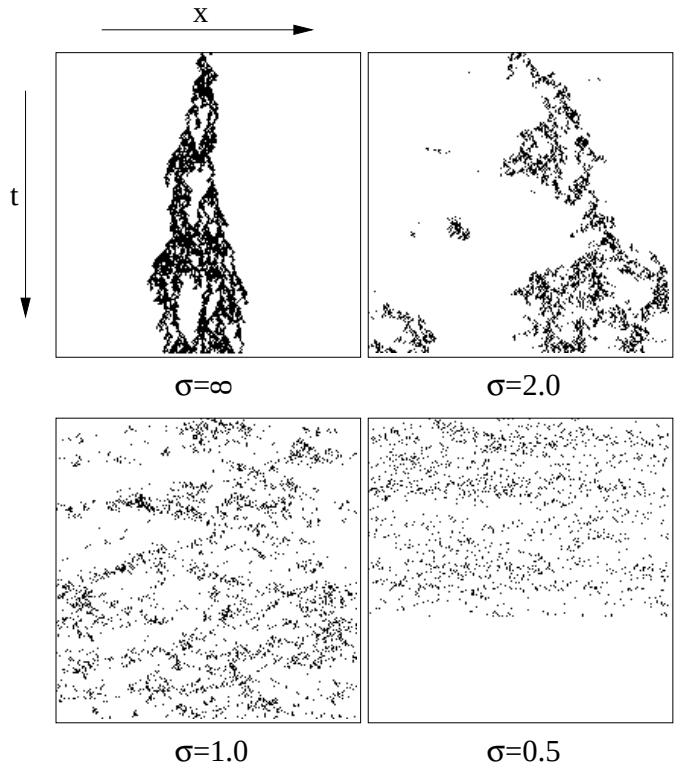

Fig. 2. Critical anomalous directed percolation in 1+1 dimensions for different values of σ. The figure shows typical clusters starting from 5 active sites in the center of the lattice. The case $\sigma = \infty$ corresponds to ordinary DP. As σ decreases, spatial structures become more and more smeared out until in the mean field limit $\sigma = 1/2$ the particles appear to be randomly distributed over the whole system. For small values of σ finite size effects may lead to sudden transitions into the absorbing state.

i.e., the particle may "revolve" several times around the system. It turns out that this simple trick considerably reduces finite size effects. In particular the value of p_c is well defined over a wide range of system sizes. Nevertheless finite size effects are still important in this model. In particular for small values of σ, where long-distance flights occur frequently, finite-size effects enhance the probability for a target site to be already occupied. This in turn reduces the average density of active sites in a growing cluster and therefore increases the probability to enter the absorbing state. For example, for $\sigma = 0.5$, a small system with only 200 sites reaches the absorbing state typically after only a few hundred time steps (see Fig. 2). Therefore, in order to further reduce finite size effects, we either use very large lattice sizes of about 10^5 sites (as in stationary simulations, see below) or else in other (dynamical) simulations, we can eliminate finite size effects almost completely by working on a virtually infinite lattice (see also below).

4 Numerical results

In order to estimate the critical exponents of anomalous DP we employ two different standard Monte-Carlo techniques, namely dynamical simulations at criticality and steady-state simulations in the active phase.

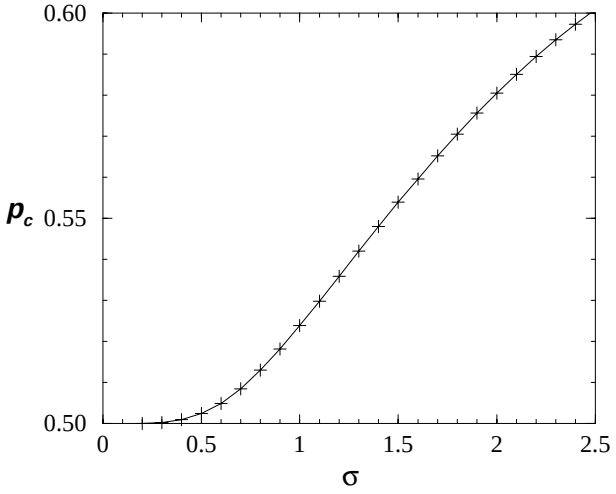

Fig. 3. The critical percolation threshold of anomalous directed bond percolation as a function of σ.

In *dynamical simulations* [19] a critical cluster is grown from a single active seed (just as in Fig. 2). Averaging over many independent realizations one measures the survival probability $P(t)$, the number of active particles $N(t)$, and the mean square spreading of surviving clusters from the origin $R^2(t)$. At criticality, these quantities are expected to scale as

$$P(t) \sim t^{-\delta}, \qquad N(t) \sim t^{\theta}, \qquad R^2(t) \sim t^{2/z}, \tag{16}$$

where $\delta = \beta/\nu_{\|}$ and θ is the critical initial slip exponent [18] (see Eq. (11)). Since the size of the growing cluster is finite, we are able to perform the simulations on a virtually infinite lattice by storing the coordinates of active particles in a dynamically generated list. The effective system size is then determined by the maximal spreading range (*i.e.*, the maximal range of integer numbers $\pm 2^{63}$), which means that finite size effects are almost eliminated. Since deviations from criticality lead to a curvature of $P(t)$ in a double logarithmic plot, the dynamical simulation method allows a precise estimate of the percolation threshold p_c for different values of σ (see Fig. 3 and Tab. 1). As expected, p_c tends to $1/2$ in the limit $\sigma \to 0$.

Having determined the critical points, we measure the quantities $P(t)$, $N(t)$, and $R^2(t)$ at criticality. However, it turns out that, in the presence of sufficiently long-range interactions, the mean square spreading, defined as an *arithmetic* average $R^2(t) = \langle |\mathbf{x}(t)|^2 \rangle$, diverges. In order to circumvent this problem, we instead compute the *geometric* average

$$R^2(t) = \exp\left[\langle \log(|\mathbf{x}(t)|^2) \rangle \right]. \tag{17}$$

This average turns out to be finite for all $\sigma > 0$ and renders consistent results in the case of ordinary DP. The numerical estimates for the dynamical exponents δ, θ, and $z/2$ are shown in Figure 4.

The exponent β is determined by *stationary simulations* in the active phase. As the active phase of anomalous

Table 1. Estimates of the percolation threshold and the critical exponents for various values of σ, compared to the corresponding values for ordinary bond DP.

σ	p_c	β	$\nu_\perp$	$\nu_\parallel$	z	θ
0.2	0.500 26(1)	0.99(4)	4.7(6)	1.00(6)	0.21(2)	0.01(3)
0.3	0.500 97(1)	0.98(5)	3.2(3)	1.01(6)	0.31(2)	0.02(3)
0.4	0.502 45(2)	0.97(6)	2.5(2)	0.99(7)	0.39(2)	0.01(3)
0.5	0.504 90(2)	0.95(6)	1.87(13)	1.01(6)	0.54(2)	0.02(3)
0.6	0.508 47(2)	0.88(5)	1.76(12)	1.02(6)	0.58(2)	0.04(3)
0.8	0.518 20(3)	0.76(4)	1.60(11)	1.13(7)	0.71(2)	0.13(3)
1.0	0.529 81(5)	0.65(3)	1.52(11)	1.25(7)	0.82(2)	0.20(3)
1.2	0.541 97(5)	0.56(3)	1.46(10)	1.40(9)	0.96(3)	0.28(2)
1.4	0.553 90(10)	0.49(3)	1.36(11)	1.48(11)	1.09(3)	0.30(2)
1.6	0.565 20(10)	0.43(3)	1.29(11)	1.56(14)	1.21(3)	0.30(2)
1.8	0.575 61(10)	0.39(3)	1.23(13)	1.62(18)	1.32(3)	0.31(2)
2.0	0.585 05(10)	0.34(3)	1.13(15)	1.62(20)	1.43(3)	0.32(2)
2.2	0.593 45(10)	0.32(3)	1.13(15)	1.68(21)	1.49(4)	0.31(2)
2.4	0.600 85(10)	0.30(3)	1.15(17)	1.76(24)	1.53(5)	0.32(2)
DP	0.644700	0.2765	1.097	1.734	1.581	0.3137

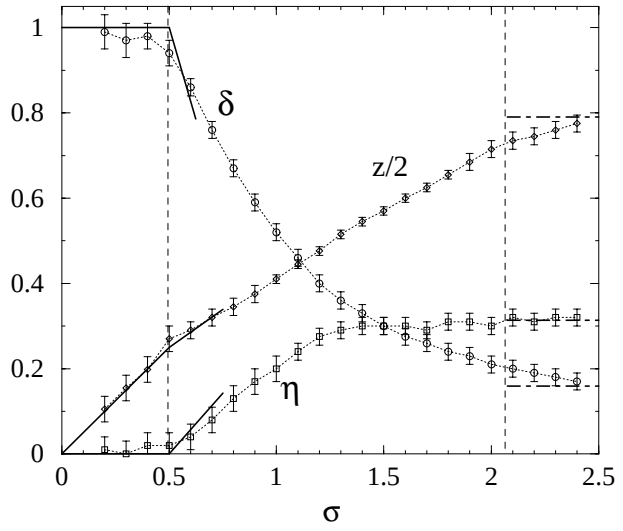

Fig. 4. Estimates for the critical exponents from dynamical Monte-Carlo simulations in comparison with the field-theoretic predictions (solid lines) and the DP exponents (dot-dashed lines).

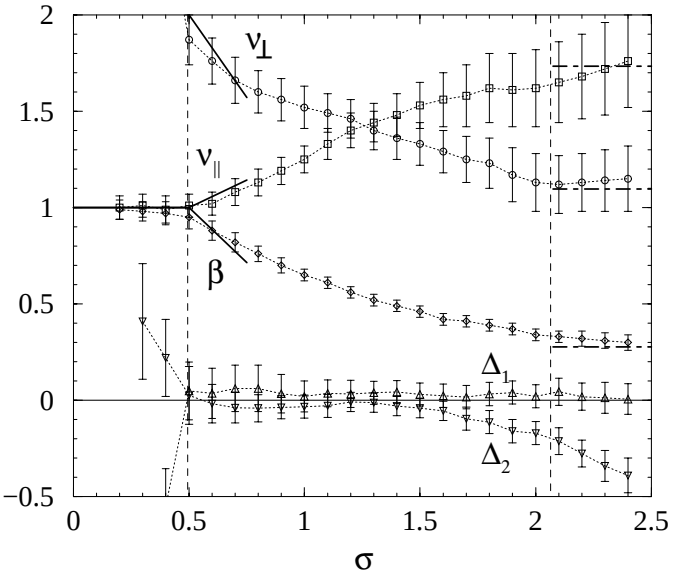

Fig. 5. Estimates for the exponent β and the derived exponents $\nu_\perp$ and $\nu_\parallel$ in comparison with the field-theoretic results (solid lines) and the DP exponents (dot-dashed lines). The quantities Δ_1 and Δ_2 represent deviations from the scaling relations (11, 13), respectively (see text).

DP is characterized by a homogeneous particle density, this type of simulation has to be performed on a finite lattice. In order to minimize finite size effects, we choose a large lattice size of $L = 10^5$ sites. Starting from a fully occupied initial state, the system first equilibrates over 10^4 time steps before the stationary density n is averaged over another 10^4 time steps. Our estimates for β are shown in Figure 5. Combining the results we can now compute the scaling exponents $\nu_\perp = \beta/\delta z$ and $\nu_\parallel = \beta/\delta$, which are summarized in Table 1.

According to equation (14), the one-loop expansion predicts the initial variation of the critical exponents close to $\sigma = 1/2$. This is one of the rare cases where one can directly "see" the field-theoretic results in the simulation data. In Figures 4, and 5, the predicted initial slopes are indicated by solid lines. Clearly they are in fair agreement with the numerical estimates, which confirms the field-theoretic results of reference [14]. For $\sigma > 1.5$, however, the numerical results are not accurate enough to verify the predicted location of the crossover to ordinary DP at $\sigma_c = 2.076\,6(2)$. It seems that the deviations in this regime are due to very long crossover times in the dynamical simulations, resulting from a complicated interplay between long-range and short-range processes.

In order to verify the scaling relations (11, 13) we have also plotted the deviations $\Delta_1 = 2\delta + \theta - 1/z$ and

$\Delta_2 = 1-\sigma+(1-2\delta)z$ which should be equal to zero in the intervals $\sigma \geq 0.5$ and $0.5 \leq \sigma \leq \sigma_c$, respectively. In fact, as shown in Figure 5, Δ_1 is smaller than the error tolerance, which confirms the validity of the hyperscaling relation (11). Similarly the values of Δ_2 confirm the validity of equation (13) in the range $0.5 \leq \sigma \leq 1.5$, whereas significant deviations occur for $\sigma > 1.5$. We believe that these deviations do not indicate that the scaling relation (13) is violated for large values of σ, rather they confirm that the simulations in this regime may be affected by very long crossover times.

5 Anomalous annihilation process

In this section we consider the somewhat simpler case of anomalous pair annihilation $A + A \to \emptyset$ with long-range hopping. This model was previously studied in [20], using both simulations and approximate theoretical techniques. In this paper we will extend this previous work, by presenting a systematic field-theoretic analysis, as well as by performing more detailed numerical simulations.

In the ordinary annihilation process [21] with short-range interactions, the average particle density is known to decay as

$$n(t) \sim \begin{cases} t^{-d/2} & \text{for } d < 2, \\ t^{-1} \ln t & \text{for } d = d_c = 2, \\ t^{-1} & \text{for } d > 2. \end{cases} \tag{18}$$

Hence, except for the log correction in $d = 2$, the density decays away as a power law, $n(t) \sim t^{-\alpha}$. Turning now to the Lévy-flight case, this may be described theoretically by inserting an additional operator ∇^σ into the well-known field-theoretic action for pair annihilation (see [21]). The resulting action reads

$$S[\bar\psi, \psi] = \int d^dx\, dt \Big\{ \bar\psi(\partial_t - D_N\nabla^2 - D_A\nabla^\sigma)\psi + 2\lambda\bar\psi\psi^2 + \lambda\bar\psi^2\psi^2 - n_0\bar\psi\delta(t) \Big\}, \tag{19}$$

where n_0 is the initial (homogeneous) density at $t = 0$. Here the field ψ is *not* simply related to the coarse-grained density field [17], although it is true that the average values of both fields are the same. The action (19) can be *derived* systematically, starting with an appropriate (non-local) Master equation — the details are given in Appendix. Note also that the action for the process $A + A \to A$ with Lévy flight hops differs only in the coefficients of the reaction terms. Hence the Lévy flight annihilation and coagulation processes are in the same universality class.

An analysis of the above action follows very closely that of reference [21]. For $\sigma < 2$, power counting reveals that the upper critical dimension of the model is now $d_c = \sigma < 2$. For $d > d_c$ mean-field theory is expected to be quantitatively accurate, with an asymptotic density decay $\sim t^{-1}$. Below the upper critical dimension, however, the renormalized reaction rate flows to an order $\epsilon = \sigma - d$ fixed point. This allows us to very quickly determine the asymptotic density decay via dimensional arguments. Below d_c the only dimensionful quantity left in the problem is the time t, which, for $\sigma < 2$, scales as $[t] \sim k^{-\sigma}$. Hence, for $\sigma < 2$, the density must decay as:

$$n(t) \sim \begin{cases} t^{-d/\sigma} & \text{for } d < \sigma, \\ t^{-1} \ln t & \text{for } d = d_c = \sigma, \\ t^{-1} & \text{for } d > \sigma. \end{cases} \tag{20}$$

The derivation of the logarithm at the upper critical dimension requires a slightly more sophisticated calculation, which is, however, completely analogous to that in reference [21]. Note also that for $\sigma \geq 2$ the results cross over smoothly to the standard annihilation exponents of equation (18).

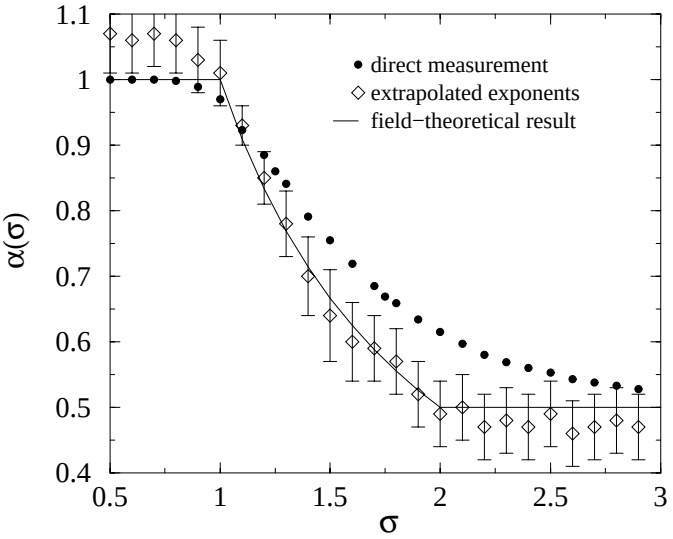

Fig. 6. The anomalous annihilation process: the graph shows direct estimates and extrapolations for the decay exponent α, as a function of σ. The solid line represents the exact result (neglecting log corrections at $\sigma = 1$).

A lattice model for anomalous annihilation in $1 + 1$ dimensions may be constructed by a simple modification of the model for anomalous DP introduced in Section 3. To this end steps 1-3 have been modified such that for all active sites i we perform the following procedure:

1. Generate a random number $z \in [0, 1]$ and define a real-valued spreading distance $r = z^{-1/\sigma}$. The corresponding integer spreading distance d is defined as the largest integer number smaller than r.
2. Generate another random number $y \in [0, 1]$ and assign $s^{new}_{i+1-2d}(t + 1) := 1 - s^{old}_{i+1-2d}(t + 1)$ if $y > 1/2$, and $s^{new}_{i-1+2d}(t + 1) := 1 - s^{old}_{i-1+2d}(t + 1)$ otherwise. As in the case of anomalous DP, the arithmetic operations in the indices are carried out modulo L by assuming periodic boundary conditions, *i.e.* $s_i \equiv s_{i\pm L}$.

In step 2 the state of the target site is simply inverted. Therefore, if two particles move to the same target site, they annihilate instantaneously.

Since the annihilation process starts with a homogeneous density of particles, it is impracticable to work with

a virtually infinite lattice by storing the coordinates of individual particles in a list. Rather we have to perform ordinary simulations with a fixed system size. In order to minimize finite size effects we choose a large lattice size of 2^{16} sites. For various values of σ we measure the particle density $n(t)$ up to 10^4 time steps averaged over at least 10^3 independent runs. By measuring the slopes of $n(t)$ in a double logarithmic plot in the decade $10^3 \leq t \leq 10^4$, we estimate the density decay exponents $\alpha(\sigma)$, which are shown in Figure 6 (labeled as direct measurements). For $\sigma < 1.5$ the agreement with the theoretical result of equation (20) (the solid line) is quite convincing, whereas large deviations occur close to $\sigma = 2$. A detailed analysis of the local slope of $n(t)$ as a function of time in a double-logarithmic plot shows that these deviations are related to very long crossover times. In fact, determining the local slopes of $n(t)$ in a log-log plot and extrapolating them graphically to $t \to \infty$, one obtains a much better coincidence. On the other hand, for $\sigma < 1$, the extrapolation leads to larger deviations. These errors may be related to finite size effects which are still extremely dominant in this regime.

6 Conclusions

In this paper we have, for the first time, studied numerically the behaviour of Lévy-flight DP close to the phase transition between the active and absorbing states. To this end, we have introduced a lattice model for anomalous DP in which finite size effects are considerably reduced. Using special simulation techniques we have obtained accurate values for the associated critical exponents in $1 + 1$ dimensions, which are almost free from finite-size effects. In addition we have performed quantitative tests of the one loop field-theoretic results, by tuning the upper critical dimension of the model to lie just above $d = 1$. Our results are all in good agreement with the recent field-theoretic analysis of [14]. Close to $\sigma = 2$, however, our numerical results are not accurate enough to confirm the form of the predicted crossover to ordinary DP. We have also considered the simpler case of Lévy-flight pair annihilation, where our numerics are again in agreement with (exact) field-theoretic arguments.

Various possible extensions of the above models are possible. The most obvious involves including a power law waiting time distribution for the particles, in addition to the power law Lévy distribution for particle hops. Hence, in the absence of interactions, each particle would perform a *continuous time Lévy flight* (see [22] and references therein). This modification should lead to a further universality class, with the exponents depending continuously on the control parameters for both the Lévy-flight and the (power law) waiting time distributions.

Appendix: Derivation of the anomalous annihilation action

In this appendix we briefly describe how the anomalous annihilation action (19) may be derived. To simplify matters we will not include the reaction terms — their derivation is precisely the same as in [21]. The appropriate Master equation for (anomalous) diffusion is given by

$$\frac{\partial}{\partial t}P(\{n\};t) = \frac{D_0}{l^\sigma}\sum_i \sum_{j(\neq i)} [(n_j+1)q_{ji} \times P(\dots, n_j+1, \dots, n_i-1, \dots; t) - n_i\, q_{ij}\, P(\{n\};t)]\,, \tag{A.1}$$

where $P(\{n\})$ is the probability of the particle configuration $\{n\} = (n_1, \dots, n_N)$, l is the microscopic lattice spacing, D_0 is the diffusion constant, and where q_{ij} gives the appropriate weight for a hop from site i to site j. Following [23], we next introduce creation and annihilation operators a_i, $a_i^\dagger$, such that

$$a_i^\dagger|n_i\rangle = |n_i+1\rangle, \qquad a_i|n_i\rangle = n_i|n_i-1\rangle, \tag{A.2}$$

with the commutator $[a_i, a_j^\dagger] = \delta_{ij}$. The system state is then given by

$$|\Phi(t)\rangle = \sum_{n_1,\dots,n_N} P(\{n\};t) a_1^{\dagger n_1} \dots a_N^{\dagger n_N}|0\rangle, \tag{A.3}$$

where $|0\rangle$ is the vacuum state. Hence we can rewrite equation (A.1) as

$$\frac{\partial}{\partial t}|\Phi(t)\rangle = -\mathcal{H}|\Phi(t)\rangle, \tag{A.4}$$

where

$$\mathcal{H} = -\frac{D_0}{l^\sigma}\sum_i a_i^\dagger \left[\sum_{j(\neq i)} (a_j - a_i) q_{ji}\right]. \tag{A.5}$$

We may now perform the mapping to a field theory using standard methods (see [23]). After taking the continuum limit in space, we end up with the continuum action

$$S = \int d^dx\; dt\; \{\hat\psi(x,t)\; \partial_t\psi(x,t) - D_1\; \hat\psi(x,t) \int d^dy \times([\psi(y,t) - \psi(x,t)] f|x-y|)\}, \tag{A.6}$$

where we have the Lévy distribution

$$f(r)\; d^dr \sim \frac{1}{r^{\sigma+d}}\; d^dr. \tag{A.7}$$

Transforming this into Fourier space, we obtain

$$S = \int \frac{d^dk}{(2\pi)^d}\; dt\; \{\tilde{\hat\psi}(k,t)\partial_t\tilde\psi(-k,t) - D_1[\tilde{\hat\psi}(k,t) \times(f(k)-1)\tilde\psi(-k,t)]\}, \tag{A.8}$$

with

$$f(k) - 1 = \frac{1}{\mathcal{N}}\int_l d^dr\; \frac{(e^{-ik.r}-1)}{r^{d+\sigma}}, \tag{A.9}$$

where $\mathcal{N}$ is a normalization constant. After some manipulation of the above integral, and after performing a small momentum expansion, we end up with

$$S = \int \frac{d^d k}{(2\pi)^d}\, dt\, \Big[\tilde{\hat{\psi}}(k,t)\partial_t \tilde{\psi}(-k,t) + \tilde{\hat{\psi}}(k,t) \times \left\{D_A k^\sigma + D_N k^2 + O(k^4)\right\} \tilde{\psi}(-k,t)\Big], \quad \text{(A.10)}$$

valid for $0 < \sigma < 4$, $\sigma \neq 2$. The final action (19) is then obtained by the inclusion of both the reaction terms, and the initial density source.

References

1. D. Mollison, J. R. Stat. Soc. B **39**, 283 (1977).
2. T.M. Liggett, *Interacting Particle Systems* (Springer, New York, 1985).
3. R. Ziff, E. Gulari, Y. Barshad, Phys. Rev. Lett. **56**, 2553 (1986).
4. E.V. Albano, J. Phys. A **27**, L881 (1994).
5. S. Havlin, D. ben-Avraham, Adv. Phys. **36**, 695 (1987).
6. J.-P. Bouchaud, A. Georges, Phys. Rep. **195**, 127 (1990).
7. W. Kinzel, in *Percolation Structures and Processes*, edited by G. Deutscher, R. Zallen, J. Adler, Ann. Isr. Phys. Soc. **5** (Adam Hilger, Bristol, 1983), p. 425.
8. P. Grassberger, K. Sundermeyer, Phys. Lett. B **77**, 220 (1978).
9. J.L. Cardy, R.L. Sugar, J. Phys. A **13**, L423 (1980).
10. H.K. Janssen, Z. Phys. B **42**, 151 (1981).
11. P. Grassberger, Z. Phys. B **47**, 365 (1982).
12. P. Grassberger, in *Fractals in physics*, edited by L. Pietronero, E. Tosatti (Elsevier, 1986).
13. M.C. Marques, A.L. Ferreira, J. Phys. A **27**, 3389 (1994).
14. H.K. Janssen, K. Oerding, F. van Wijland, H.J. Hilhorst, Eur. Phys. J. B **7**, 137 (1999).
15. E.V. Albano, Europhys. Lett. **34**, 97 (1996).
16. S.A. Cannas, preprint cond-mat/9711297.
17. M.J. Howard, U.C. Täuber, J. Phys. A **30**, 7721 (1997).
18. H.K. Janssen, B. Schaub, B. Schmittmann, Z. Phys. B **73**, 539 (1989); H.W. Diehl, U. Ritschel, J. Stat. Phys. **73**, 1 (1993); F. van Wijland, K. Oerding, H.J. Hilhorst, Physica A **251**, 179 (1998).
19. P. Grassberger, A. de la Torre, Ann. Phys. (N.Y.) **122**, 373 (1979).
20. G. Zumofen, J. Klafter, Phys. Rev. E **50**, 5119 (1994).
21. B.P. Lee, J. Phys. A **27**, 2633 (1994).
22. H.C. Fogedby, Phys. Rev. E **50**, 1657 (1994).
23. L. Peliti, J. Phys. France **46**, 1469 (1985).